Numerical investigation on the performance of a small scale solar chimney power plant for different geometrical parameters

Ekin Özgirgin Yapıcı [*], Ece Ayli , Osama Nsaif

Çankaya University, Department of Mechanical Engineering, 06790, Ankara, Turkey

ABSTRACT

In recent decades, demand for energy has been significantly increased, and considering environmental impacts and the degrading nature of fossil fuels, clean and emission-free renewable energy production has attracted a great deal of attention. One of the most promising renewable energy sources is solar energy due to low cost and low harmful emissions, and from the 1980s, one of the most beneficial applications of solar energy is the utilization of solar chimney power plants (SCPP). A SCPP is a simple and reliable system that consists of three main components; a solar collector, a chimney (tower) and a turbine to utilize electrical energy. Recently, by the advancement in computer technology, the use of CFD methodology for studying SCPP has become an extensive, robust and powerful technique. In light of the above, in this study, numerical simulations of a SCPP through three-dimensional axisymmetric modeling is performed. A numerical model is created using CFD software, and the results are verified with an experimental study from the literature. After ensuring good agreement with the experiments, chimney's and collector's geometric parameters effects and different configurations effects on SCPP performance, simultaneously and additively is investigated. The study introduces an insight to the performance enhancement methods and finding the best configuration of a SCPP model, which will be the basis of a detailed prototyping process. Based on the numerical results, the best configuration of the SCPP has been found as the diverging chimney which enhances the generated power. The results of the study showed that the chimney height and collector radius increase has a positive effect on the power output and efficiency of the system, but when construction and material costs are also considered, each has an optimal value. The maximum impact on the performance is found to be by the chimney tower radius and the collector height and inclination are found to have optimum values considering performance. According to the obtained results, the best performance for the SCPP was obtained with 3.5 m chimney height, 30 cm tower diameter, 400 cm of collector diameter with 6 cm height and zero inclination angle. By the correct selection of the dominant performance parameter which can be done by correctly interpreting the results of this study, "the best" design of a SCPP real scale prototype considering maximum power requirement can be done.

© 2020 Elsevier Ltd. All rights reserved.

1. Introduction

Reducing the use of fossil fuels, thus, reliance on renewable and clean energy sources has become one of the primary objectives of governments and also partly the private sector in the global economy. By degradation of fossil fuels, since the demand for sustainable energy increases, it becomes necessary to search for efficient power generation applications based on clean energy sources.

One of the most promising sources of clean energy is solar energy regarding low cost and no harmful emissions. Among solar technologies, solar chimney power plant (SCPP) has gathered great interest in the utilization of solar energy. The solar chimney power plant is a system that produces electricity with the help of the wind turbine placed in the center of the chimney, driven with airflow generated by buoyancy resulting from the greenhouse effect inside the collector. It consists of three main components: The solar collector, chimney and wind turbine.

The collector absorbs solar radiation, and in this way, the air between collectors and absorber is heated. The air is moved as a result of buoyancy and density change between warm air and the

---

Nomenclature

A	Flow Area [m^2]
D_M	Chimney Diameter [m]
D_L	Chimney Radius [m]
H_{ch}	Chimney Height [m]
H_c	Collector Height [m]
h	Heat transfer coefficient [W/m^{2}K]
$\dot{m}$	Mass flow rate [kg/s]
P_{out}	Power Output [W]
V	Air velocity [m/s]

Greek Symbols

ρ	Density [kg/m^3]
β	Inclination Angle [ ]
ε	Emissivity of Sunroof [-]

---

ambient air. This air flow passes through a wind turbine which leads to the generation of electricity since it is coupled to a generator. The geometrical parameters such as chimney radius, collector size, ambient conditions, collector and chimney material including glazing and insulation have direct effects on the solar chimney efficiency and the amount of electricity production. Optimization of the geometric parameters to find the best configuration in order to exploit solar energy is very crucial for solar chimneys.

SCPPs have many advantages since they are suitable for electricity generation in deserts and sun-rich wastelands with no significant fuel demand. They are environmentally friendly, give no ecological harm. Conservation of water is another advantage of SCPPs, because they don't need cooling water. The air collector can absorb both beam and diffused radiation so that the SCPP can operate on both clear and cloudy days. The collector is a natural thermal energy storage system, as the ground under the cover absorbs some of the radiated energy during the day and releases it at night to produce some amount of electricity as well. It also has a low construction cost.

In last decades, researchers and companies have become increasingly interested in the solar chimney because of its many advantages. As a result, many numerical and experimental studies for SCPPs are done all over the world. All these studies and prototype sought to estimate the efficiency of the SCPPs in different environmental conditions and variable dimensions in a try to reach the highest performance and efficiency for SCPP. Most of the simulation studies are based on analyzing the results and comparing them with the model found in Manzanares prototype. These studies provide a complete picture of SCPPs and clearly show the factors affecting on SCPP performance. These studies provide the groundwork for researchers to work on developing an optimal design of SCPP and building a highly efficient commercial solar chimney power plants (Al-Dabbas, 2011; Dai et al., 2003). Bernardes et al. (2003) studied the impact of external factors and change of parameters like the height of the chimney and the difference in pressure at the entry and exit of the system and the collector properties. According to results, it is claimed that the collector diameter has a direct effect on the efficiency of the system. Al-Kayiem et al. (Al-Kayiem and Aja, 2016) showed that the amount of solar radiation, type of absorption material, the top layer of the solar collector and the tilt angle of the collector have a significant effect on solar chimney performance.

In the work of Maia et al. (2009), the effect of airflow within the system is studied with numerical methods, and it is found that the height and the diameter of the chimney are the most important variables, which increase the efficiency of the system, but may also affect the cost of the power plant. Due to Zhou et al. (2007), increasing the chimney height and collector diameter raises the generated power. Also, Fasel et al. (2013), obtained similar results with Zhou et al. (2007), that increasing the chimney height has a positive effect on the solar chimney efficiency.

The study of Li et al. (2016), observed that the height of the solar collector and the thickness of the absorption layer have a limited effect on the performance of SCPP. Kasaeian et al. (Zhou et al., 2009), showed that the chimney diameter and chimney height have a positive effect on increasing efficiency, while the diameter of the chimney has a predominant effect on chimney performance. Fathi et al. (2018), used the surplus heat from the nuclear cycle to enhance the efficiency of the solar chimney power plant. Their results depicted that using the wastewater heat of the nuclear power plant and generating a combined cycle, increases the SCPP efficiency from 35.3% to 42%. Amudam et al. (Amudam and Chandramohan, 2019), developed a 3D model of SCPP with and without a thermal energy storage system. They compare performance parameters with each other numerically. It was found that the thermal storage system increases the total generated power as this system dissipates the stored heat to incoming air when there was no solar radiation. Okoye (2016), optimized the SCPP dimension regarding maximizing the power and minimizing the cost. They claimed that the economic feasibility of SCPP improves with increasing plant dimensions. Also insight into the results, it is seen that for constant energy demand, increasing efficiency decreases the optimal SCPP dimensions and total cost. Hu et al. (2017), numerically studied many types of chimney geometries based on the influence of increasing the upper radius of tower on the driving potential of the SCPP. In this study, cylindrical chimney, divergent outlet chimney (DOSC), divergent inlet chimney (DISC) and divergent chimney (DSC) are examined and their aerodynamic characteristics and their ability to generate power were revealed. The simulation results showed that the DSC has a better effectiveness for the power production than the cylindrical SC which it is almost higher by 13.5 times than the cylindrical tower and increasing in power with the DISC in the range from 2 to 10 times, while the DOSC increasing at maximum to about 5 times. Bouabidi et al. (2018), presented a numerical model to study the effect of the chimney configurations on SCPP performance and to simulate the airflow inside SCPP. For the numerical analysis of the SCPP, four types of tower geometries; standard, divergent, convergent and opposing tower are studied. The results indicated that the chimney geometry has a significant influence on the changing of the velocity behavior which occurs due to the pressure distribution resulted from the variation of chimney geometry. The SCPP performance is enhanced with the divergent and opposing tower by the increase of velocity and maximum velocity appears at divergent geometry.

Li et al. (2012), evaluated the performance of an SCPP through a theoretical model and the results have been validated by the data of the Manzanares SCPP in Spain. The theoretical model studies the effects of airflow and thermal losses and the rate of temperature changes at the tower. Depending on the solar radiation there is the highest power range for the solar chimney for specific solar irradiation values due to the effect of the installation of the turbines, flow and heat losses inside SCPP. A solar power plant with a shorter diffuser is firstly patented and examined by Ninic and Nizwtic (Nizetic, 2011; Ninic and Nizetic, 2007). They claimed that a plant with shorter diffuser have higher efficiency and will be less costing. Also, Penga et al. (2019), numerically investigated the concept of a solar power plant with short diffuser and they optimized the guide vane topology to decrease the required pressure potential that is crucial for stable operation of the SDP plant. Their first study

showed that the CFD tool is compromising and capable to analyze the stable vortex structure (Nizetic et al., 2017). The results indicate that guide vane shape has a dominant effect on the swirl ratio, and the swirl ratio is independent of the Reynolds number.

In the light of above, the aim and motivation of this study is to investigate multiple geometric parameters effects and different configurations effects on SCPP performance, simultaneously and additively, introduce an insight to the performance enhancement methods and find the best configuration of a SCPP considering all parameters effects. For this reason, a numerical model of the SCPP through three-dimensional axisymmetric modeling by using CFD software is created. Numerical results are verified with an experimental study from the literature. After ensuring good agreement with the experiments, performance enhancement methods for SCPP are investigated.

For this study, the best model will then be used to further investigate the chimney performance experimentally to study the performance parameters of the chimney, the wind turbine, electricity production, and coupling as future work. Also with the help of nondimensionalizing which is explained in later chapters, prototypes of real sized solar chimneys will be possible to construct using the currently studied chimney as the model, considering the most effective parameter as the geometric similarity scale factor for non-dimensional optimization.

The schematic outline of the paper is given in Fig. 1. The outline of the paper is presented as follows. After the introduction and literature survey given in Section 1; mathematical and numerical methodology of SCPP is briefly explained in section 2. System description, assumptions, boundary conditions, numerical methodology, meshing effect is also examined in this part.

In Section 3, firstly validation of the model is done, then, the effect of geometrical parameters on SCPP power output and performance are studied. The paper is summarized with important remarks in Section 4, the conclusion part.

According to the authors' knowledge, there has been no study which both investigates the different chimney configurations and chimney geometric parameters' effect on SCPP performance at the same time. This study introduces an insight into the solar chimney performance under different chimney height, chimney radius, different collector parameters and different geometrical configurations of the chimney. Most important of all, by simulating a great number of cases considering a variety of parameters, most influential and less influential effecting parameters are also determined. Since for the design of real systems, such detailed studies are required for finding the best performance model.

2. Methodology

2.1. Mathematical modelling of SCPP

Equations regarding flow rates, pressure differences, performance parameters, and efficiency values for the collector, chimney and the turbine are given in detail in this part of the study. In order to simulate the SCPP, several assumptions have been considered as provided below:

- The steady-state condition is assumed for the entire analysis since the system is operating for long hours under same conditions
- Air is assumed as an ideal gas and incompressible since average temperature and pressure of air during the operation is not close to critical properties and velocity of air in the system is fairly low.
- Chimney tower is perfectly insulated-adiabatic boundary conditions are assumed for the simplicity of the solution to the problem as approached by other studies (Al-Dabbas, 2011; Zuo et al., 2020).
- The pressure at the inlet of the collector is atmospheric, as the solar chimney system is prone to atmosphere. Thermodynamic model of the solar chimney can be seen in Fig. 2.

The performance of the solar collector is based on the following equations (Thakre et al., 2013). The efficiency of the collector can be calculated by;

$$\eta_{coll} = \frac{\dot{Q}}{A_{coll}\,G} \tag{1}$$

where A_{coll} is the collector surface area (m^2), and G is the solar radiation (W/m^2) since;

$$\dot{Q} = \dot{m}\,C_p\,\Delta T \tag{2}$$

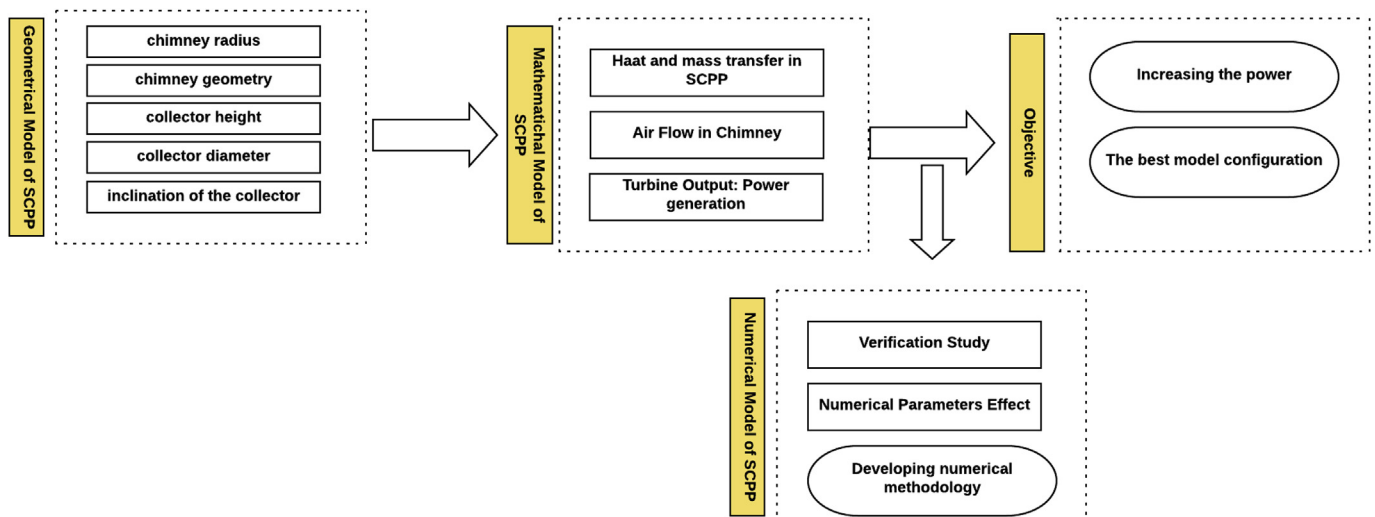where $\dot{m}$ is the mass flow rate of air (kg/s), c_p is the specific heat

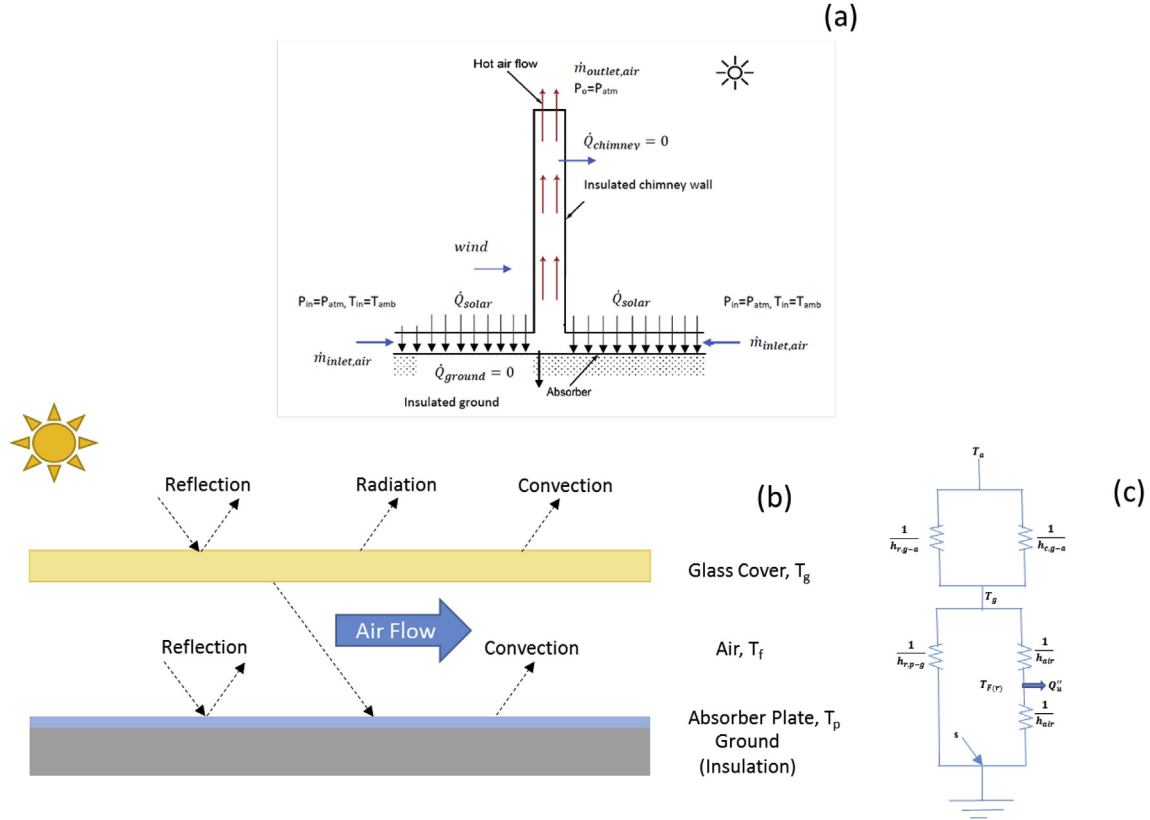**Fig. 1.** Schematic overview of the research.

Fig. 2. (a) The thermodynamic model of the SCPP (b) Energy flow through control volume of SCPP (c) Thermal resistance network for collector-plate region.

capacity of air (kJ/kg. K) and ΔT is the temperature difference (K). Applying the continuity equation, efficiency can be written as;

$$\eta_{coll} = \frac{\rho_{ch}\, v_{ch}\, A_{ch}\, C_p\, \Delta T}{\pi\, R_{coll}^2 \Delta G} \tag{3}$$

where ρ_{ch} is the density of air at the chimney inlet (kg/m³), v_{ch} is air velocity at chimney inlet (m/s) and A_{ch} is the cross-sectional area of the chimney (m²). ΔT is the temperature difference between ambient and inlet of the tower. The overall pressure difference between the chimney base and the outlet of the chimney can be calculated as (Zhou et al., 2009);

$$\Delta p = \Delta p_t + \Delta p_f + \Delta p_{in} + \Delta p_{out} = 0.00353\, H.\left(\frac{\pi\, G\, \eta_{coll}^2}{c_p\; \dot{m}}\, R_{coll}^2 - \frac{g}{2\, c_p}\, H + \frac{1}{2}\, \gamma_\infty\, H \right); \tag{4}$$

where.

$\Delta p_f = f\, \frac{H}{D}\, \frac{1}{2}\, \rho\, V^2$ is the friction loss, $\Delta p_{in} = \varepsilon_{in}\, \frac{1}{2}\, \rho\, V^2$ is the entrance loss;

$\Delta p_{out} = \varepsilon_{out} \frac{1}{2}\, \rho_{out}\, V_{out}^2$ is the exit kinetic energy loss and Δp_t = Pressure difference at the turbine, all in Pascal. In Eq. (4), γ_∞ is the lapse rate of atmospheric air temperature which can be neglected. In the case of a turbine, which will be experimentally investigated in the scope of the further studies, turbine power is calculated as (Thakre et al., 2013);

$$\dot{W}_{out} = \eta_T.\eta_{tg}\, \Delta p_t\, .\, V_{ch,max}.\, A_{ch} \tag{5}$$

The maximum value of velocity in the chimney can be calculated with the below equation;

$$V_{ch,max} = \sqrt{\frac{2\, g\, H_{ch}\, \Delta T}{T_0}} \tag{6}$$

where η_T is the turbine isentropic efficiency and η_{tg} is the efficiency of the turbine generator, and T_0 is the ambient temperature.

Finally, for the real turbine, the total conversion efficiency can be found by;

$$\eta = \frac{\dot{W}_{out}}{A_{coll}\, G} \tag{7}$$

The energy conservation principle is applied to the SCPP parts. In Fig. 2, energy exchange process is depicted. Radiation exchange, the gain or loss of enthalpy, energy gain by air surrounding and the chimney by convection heat transfer, incident radiation are shown in the thermal resistance system.

2.2. Numerical modelling of SCPP

The numerical modeling is done using ANSYS-Fluent (FLUENT), based on one of the data sets from the experimental work of Ghalamchi et al. (2016), with 0.2 m chimney diameter, 3 m chimney height, 1.5 m collector diameter and 0.06 m collector height. In the scope of the study first, 3D geometrical model of SCPP is built; then boundary conditions are applied. After the mesh independency and turbulence model studies, model verification is done and finally different cases for chimney height (H_{ch}), chimney diameter (D_{ch}), collector height (H_c), collector radius (R_c), collector inclination angle(β) and chimney geometry effects on the solar chimney performance are investigated.

To simulate the heat transfer and fluid flow distribution inside the SCPP, the flow is considered to be two-dimensional, steady-state, incompressible and viscous flow. The flow within solar chimney could be described by the Navier-Stokes equations, which consist of continuity, momentum, and energy transport equations. The governing equations are as follows (Wilcox, 2006; Cao et al., 2018):

2-D, steady state continuity equation is given by Eq. (8):

$$\frac{\partial(\rho u)}{\partial z} + \frac{1}{r}\frac{\partial(r\rho v)}{\partial r} = 0 \tag{8}$$

2-D, steady state momentum equations are written as follows:

$$\frac{\partial(\rho uu)}{\partial z} + \frac{1}{r}\frac{\partial(r\rho uv)}{\partial r} = \frac{\partial p}{\partial z} + (\rho - \rho_0)g + 2\frac{\partial}{\partial z}\left[(\mu + \mu_t)\frac{\partial u}{\partial z}\right] + \frac{1}{r}\frac{\partial}{\partial r}\left[\right.$$
$$\left. \times (\mu + \mu_t)r\left(\frac{\partial u}{\partial z} + \frac{\partial v}{\partial r}\right)\right] \tag{9}$$

$$\frac{\partial(\rho uv)}{\partial z} + \frac{1}{r}\frac{\partial(r\rho vv)}{\partial r} = -\frac{\partial p}{\partial r} + \frac{\partial}{\partial z}\left[(\mu + \mu_t)\left(\frac{\partial v}{\partial z} + \frac{\partial u}{\partial r}\right)\right] + 2\frac{1}{r}\frac{\partial}{\partial r}\left[\right.$$
$$\left. \times (\mu + \mu_t)r\frac{\partial v}{\partial r}\right] - \frac{2(\mu + \mu_t)v}{r^2} \tag{10}$$

The energy equation is given by Eq. (11):

$$\frac{\partial uT}{\partial z} + \frac{1}{r}\frac{\partial(rvT)}{\partial r} = -\frac{1}{\rho} + \frac{\partial}{\partial z}\left[\left(\frac{\mu}{Pr} + \frac{\mu_t}{\sigma_t}\right)\frac{\partial T}{\partial z}\right] + \frac{1}{\rho r}\frac{\partial}{\partial r}\left[\right.$$
$$\left. \times \left(\frac{\mu}{Pr} + \frac{\mu_t}{\sigma_t}\right)r\frac{\partial T}{\partial z}\right] \tag{11}$$

The k-ϵ turbulence model is incorporated for describing the airflow created by the buoyancy force inside the chimney according to the results of the turbulence model study. The turbulent kinetic energy equation is written as follows:

$$\frac{\partial}{\partial t}(\rho k) + \frac{\partial(\rho k u_j)}{\partial x_j} = \frac{\partial}{\partial x_j}\left(\left(\mu + \frac{\mu_t}{\sigma_k}\right)\frac{\partial k}{\partial x_j}\right) + G_k + G_b - Y_M - \rho_\varepsilon + S_k \tag{12}$$

The dissipation rate of the turbulent kinetic energy equation is written as follows:

$$\frac{\partial}{\partial t}(\rho\varepsilon) + \frac{\partial(\rho\varepsilon u_j)}{\partial x_j} = \frac{\partial}{\partial x_j}\left(\right.$$
$$\left. \times \left(\mu + \frac{\mu_t}{\sigma_\varepsilon}\right)\frac{\partial\varepsilon}{\partial x_j}\right) + \rho C_1 S_\varepsilon + \rho C_2\frac{\varepsilon^2}{k + \sqrt{\vartheta\varepsilon}} + C_{1\varepsilon}\frac{\varepsilon}{k}C_{3\varepsilon}G_b + S_\varepsilon \tag{13}$$

where G_k and G_b are the generations of turbulence kinetic energy due to mean velocity gradients and buoyancy respectively (Nasraoui et al., 2020). The discrete ordinate model (DO) is selected to compute the incident solar irradiation on the semi-transparent collector walls.

In the numerical solution, the PRESTO scheme is used, and the second-order upwind scheme is chosen. The standard algorithm is used to discretize the pressure equation, and a SIMPLE algorithm is chosen to couple the velocity and pressure fields. To compute the gradients, the Green-Gauss Cell-Based method is used. The computations are performed with a maximum residual of 10^{-6} and a maximum number of iterations of 20,000.

2.2.1. Physical domains, boundary conditions

For the numerical study, a schematic configuration of the physical model and boundary conditions are given in Table 1 and Fig. 3(a). Pressure inlet and pressure outlet conditions are utilized in the inlet and outlet of the domain respectively. An adiabatic wall with zero heat flux is considered at the chimney height. For collector roof and absorber semi-transparent wall is utilized with the amount of solar radiation of 850 W/m^2, which is the same with the experimental study, and since collector glass emissivity is 0.9, heat flux on the wall is 765 W/m^2. The Boussinesq approximation is used for modeling the buoyancy-driven flow, absorber emissivity is 0.55, and the chimney is assumed to be entirely black.

The physical domain of the SCPP is prepared using ANSYS Geometry module. The first case is considered as the base case that has same fluid and geometrical properties as Ghalamchi et al. (2016). The obtained geometry is shown in Fig. 3 (b).

2.2.2. Meshing and turbulence model effect

For mesh independency study, four different hexahedral mesh structures are prepared with 5×10^5, 1×10^6, 1.5×10^6 and 2×10^6 elements. The near-wall region has a 15-layer denser grid to deal with fast changes within the near wall. Mesh independency test results are presented as a function of temperature distribution through the collector. Temperature values are obtained for eight different collector locations. In Fig. 3(c) and (d) mesh structures are depicted for standard and divergent chimney with inclination. Also in Fig. 4 (d) and (e), 3D mesh structure can be seen for divergent chimney. Grid independency is achieved by increasing the number of elements and plotting convergence of temperature distribution for all cases, as it is shown in Fig. 4 (a). Concerning the results, after 10^6 number of mesh elements, values are almost the same for all of the locations, and RMS errors decrease to % 1.27 for the maximum point. Therefore considering the computational costs as well, using one million mesh elements is found to be appropriate for the solution to this problem.

After achieving mesh independency results, a turbulence model study is performed. In the literature, mostly k-ω and k-ε models are utilized for the solution of such problems (Nasraoui et al., 2020; Fallah and Valipour, 2019). Considering that, these two models are used and compared for the turbulence model study. As it is depicted in Fig. 4 (b), k-ε turbulence model gives a better approach than k-ω when they are compared with experimental data. Especially in the middle region of the collector, k-ω model

Table 1
Description of the boundary conditions.

Boundary Condition	Type		Parameters
	Optical	Thermal	
Collector Inlet	–	Pressure Inlet	$T_0 = 302$ k
Chimney Outlet	–	Pressure Outlet	$P_0 = 0$ Pa
Chimney Wall	Opaque Wall	Heat Flux (Adiabatic Wall)	$Q = 0$ W/m^2
Absorber	Opaque Wall	Heat Flux	$Q = 765$ W/m^2
Down Roof	Semi-transparent wall	Coupled	–
Top Roof	Semi-transparent wall	Mixed	$h = 5$ W/m^{2}K
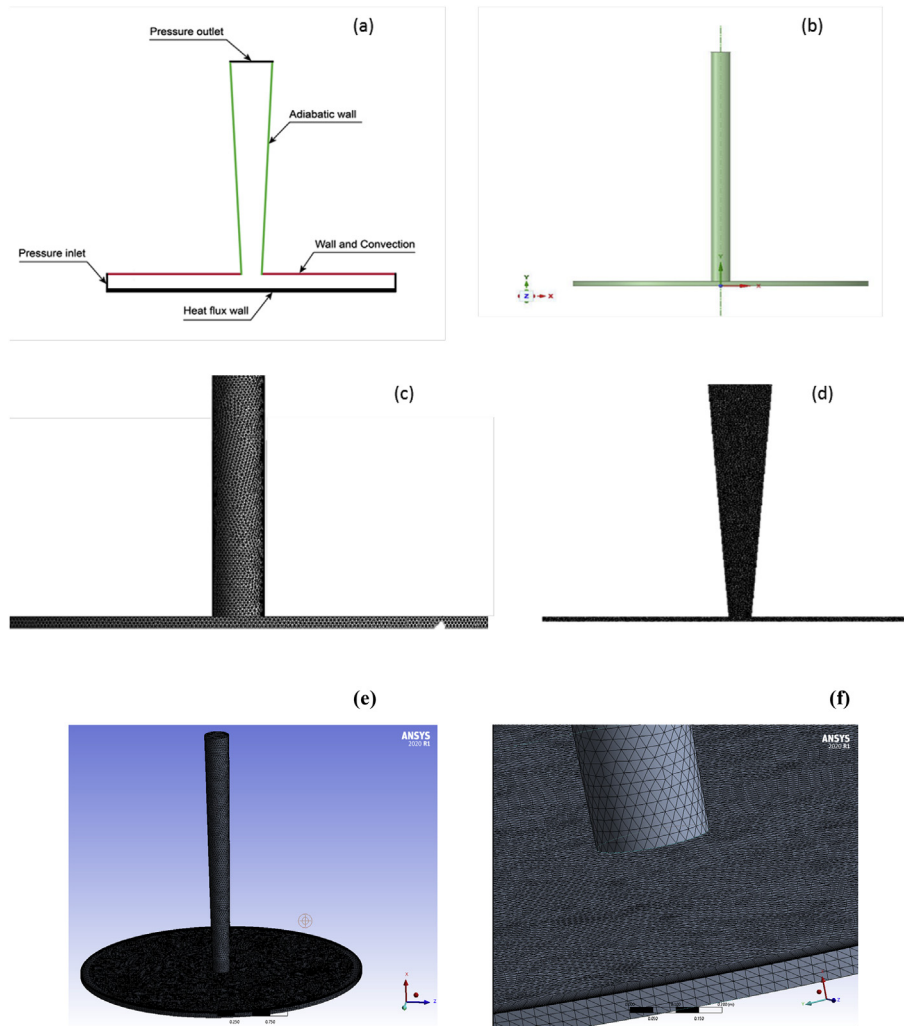
Fig. 3. (a) Schematic view of the boundary conditions (b) Generated simulation domain (c) Mesh of the standard chimney (d) Mesh of the divergent chimney (e) Mesh of the chimney in 3D (f) Detailed mesh structure of the chimney in 3D.

overestimates the temperature values.

2.2.3. Test cases

CFD simulations for different cases have been performed with varying velocity values between 0.1 and 1.6 m/s, corresponding maximum Reynold's number is around 17500. Rayleigh number is approximately 8×10^8 which indicates that the flow is turbulent. Temperature values are ranging between 305 and 330 K. In Table 2, 3, 4 and 5, and Figs. 5–7, different configurations of different cases under study and illustrations of the cases are summarized.

From Case 1 to Case 7, chimney configuration 1 is used for studying chimney tower dimension effects. After that, from Case 6-a to Case 6-b, different geometries for chimney towers are studied. Finally, for the cases from 8 to 15, chimney configuration 2 is used for studying collector dimension effects; from cases 12- to 12-c, again for the chimney configuration 2, collector inclination effects are studied.

3. Results and discussion

In the scope of this study, effects of geometric parameters which are given in Tables 2–5 are investigated on solar chimney
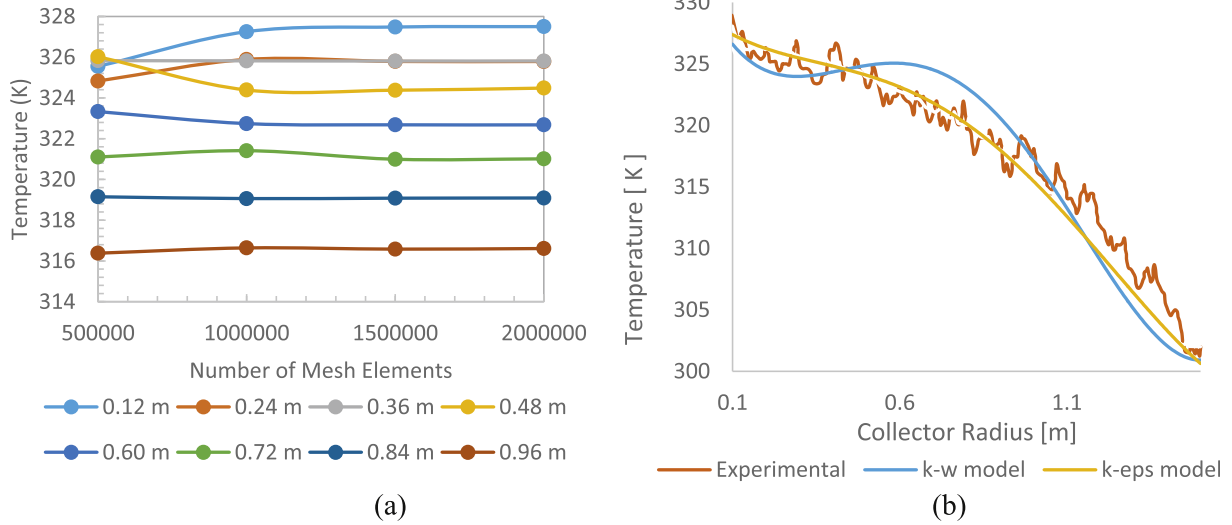
Fig. 4. (a) Mesh independency study (b) Turbulence model study.

Table 2
Solar chimney configurations for different cases; studying chimney parameters (Height and diameter).

Case	Chimney Tower Parameters		Collector Parameters	
	H_{ch} (cm)	D_{ch} (cm)	R_c (cm)	H_c (cm)
1 (Verification Case)	300	20	150	6
2	150	20	150	6
3	250	20	150	6
4	350	20	150	6
5	350	15	150	6
6	350	25	150	6
7	350	35	150	6

Table 3
Different solar chimney configurations regarding to the geometries.

Case	Chimney Tower Parameters					Collector Parameters	
	H_{ch} (cm)	D_{ch} (cm)	D_U (cm)	D_M (cm)	D_L (cm)	R_c (cm)	H_c (cm)
6-a	350	25	–	–	–	150	6
6-b	350	25	35	–	25	150	6
6-c	350	25	35	25	35	150	6
6-d	350	25	35	25	25	150	6

Table 4
Solar chimney configurations with different collector radius and height.

Case	Chimney Tower Parameters			Collector Parameters		
	H_{ch} (cm)	D_M (cm)	D_L (cm)	R_c (cm)	H_c (cm)	β (°)
8	350	35	25	100	6	0
9	350	35	25	125	6	0
10	350	35	25	150	6	0
11	350	35	25	175	6	0
12	350	35	25	200	6	0
13	350	35	25	200	4	0
14	350	35	25	200	8	0
15	350	35	25	200	10	0

Table 5
Solar chimney configurations for different cases studying collector inclination.

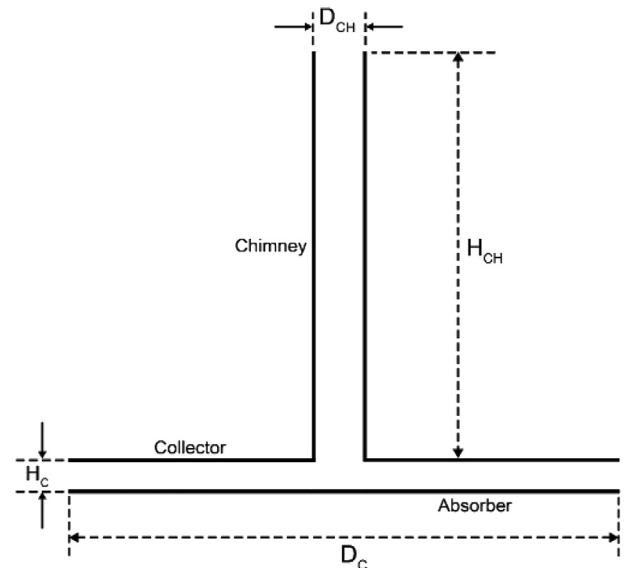| Case	Chimney Tower Parameters			Collector Parameters		
	H_{ch} (cm)	D_M (cm)	D_L (cm)	R_c (cm)	H_c (cm)	β (°)
12	350	35	25	200	6	0
12-a	350	35	25	200	6	0.5
12-b	350	35	25	200	6	−0.5
12-c	350	35	25	200	6	−1

Fig. 5. Schematic overview and parametric representation of the solar tower.

- Case 1: Comparison of experimental results with the numerical study (numerical methodology developed with this case)
- Case 1- Case 4: **Variable chimney height**, fixed chimney radius, fixed collector radius, fixed collector height
- Case 4- Case 7: Fixed chimney height, **variable chimney radius**, fixed collector radius, fixed collector height
- Case 6-a- Case 6-d: Chimney geometry is changed with varying the chimney diameters forming **different geometries.**
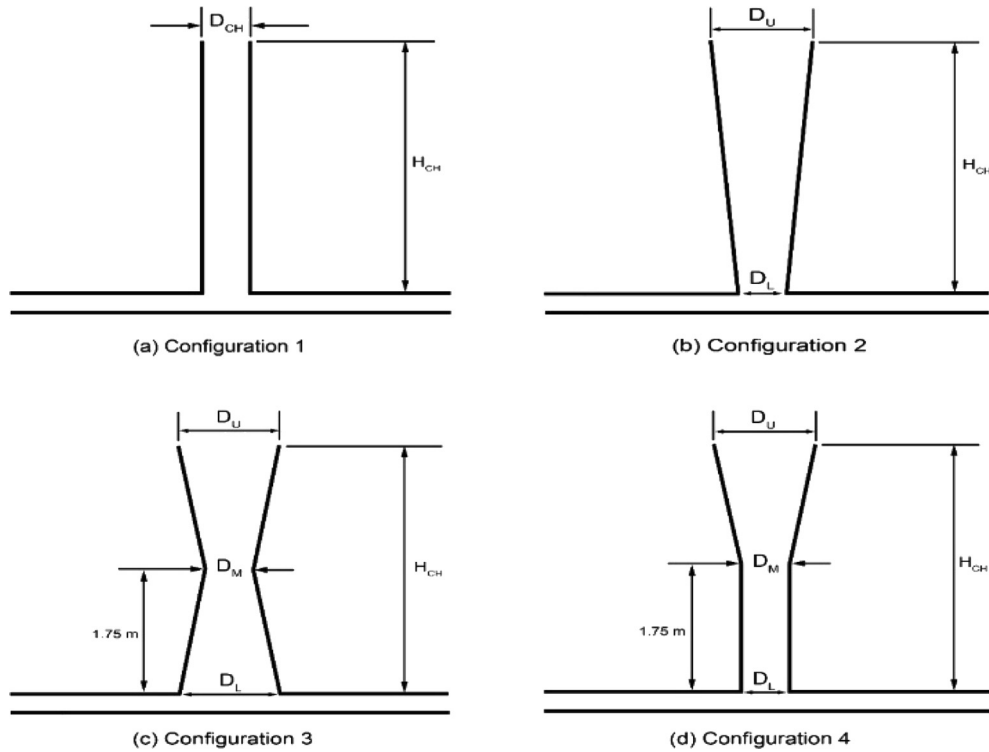
performance, after the verification of the numerical methodology by comparing experimental results and numerical results (Case 1). As a summary:

Fig. 6. Parametric view of the different solar chimney configurations regarding to the geometries. (a) Case 6-a (b) Case 6-b (c) Case 6-c (d) Case 6-d.
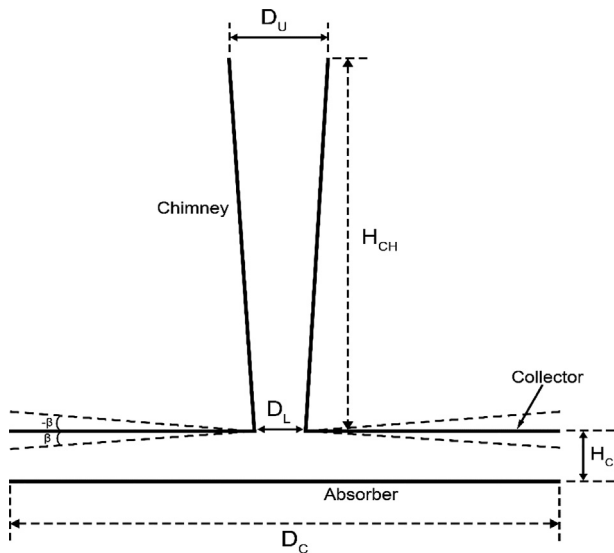

Fig. 7. Parametric view of the solar chimney with different collector dimensions (Case 8-Case 15).

- Case 8- Case 12: Fixed chimney height, fixed chimney radius, **variable collector radius**, fixed collector height
- Case 12- Case 15: Fixed chimney height, fixed chimney radius, fixed collector radius, **variable** collector height
- Case 12 - Case 12-c: Fixed chimney height, fixed chimney radius, fixed collector radius, fixed collector height, **variable inclination angle of collector roof**

For all the cases, pressure, velocity, and temperature contours are obtained; velocity and temperature distributions through

collector radius are determined. For comparison between the different cases, available power values considering the presence of wind turbines in the middle of the collector, regarding pressure drop among the turbine are derived using Eq. (5). Temperature values, velocity values (including maximum velocity in the tower), and dimensions are taken from CFD simulation results.

3.1. Verification of the base case

Using of one million mesh elements and k- ε turbulence model, verification of the numerical model has been done by comparing the numerical model with one of the data sets from cases conducted experimentally by Ghalamchi et al. (2016). The case has 0.2 m chimney diameter, 3 m chimney height, 1.5 m collector diameter, and 0.06 m collector height as already mentioned and the temperature and velocity distribution through collector radius found numerically and which was found by experimental methods can be seen in Fig. 8 (a) and (b).

Based on the results obtained from the numerical simulations, maximum relative mean errors are less than 6.4% and 4.5% for temperature and velocity distributions, respectively.

3.2. Influence of solar chimney height on SCPP performance

In the current study, the chimney tower heights are considered between 150 cm and 350 cm, as shown in Table 1. As it can be seen from Fig. 9 (a) and (b), increasing the chimney height rises both temperature and velocity values but has a more dominant effect on velocity then temperature.

According to Fig. 10, in the center of the chimney, high-velocity zone gets slightly more significant with increasing chimney height. Higher velocity values led to increase in the flow rate but reduce the temperature at the collector unit. Due to the ideal gas equation of state, increasing velocity and temperature causes a decrease in the
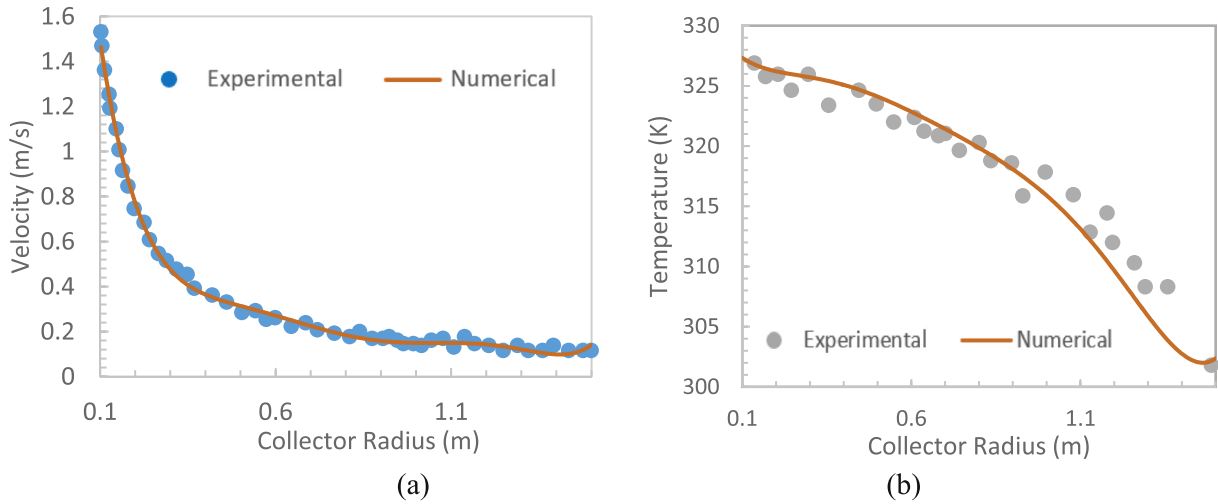
Fig. 8. Comparison of numerical and experimental results (Case 1) (a) Velocity (b) Temperature.
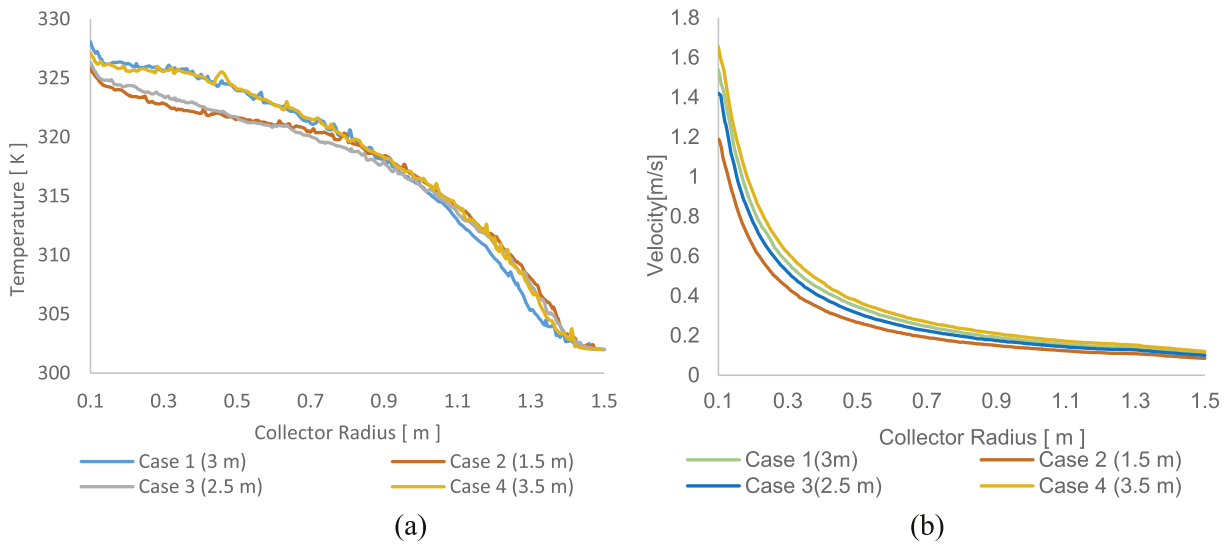

Fig. 9. Effect of chimney height on plant performance (a) Temperature distribution (b)Velocity distribution among the collector radius.

pressure values. Therefore, it can be concluded that maximum velocity will ensure the maximum power output of the system.

When power vs. chimney height graphic in Fig. 11 is examined, it is clearly seen that, before reaching a critical chimney height (which is about 3.4 m for this special case), increasing the height rises the power gradually due to increase in the mass flow and velocity. However, after reaching this critical point, further increasing the chimney height, losses its dominant effect on power values. Due to Najm et al. (Najm and Shaaban, 2018), chimney height has a direct effect on turbine efficiency, as shown in Fig. 11,
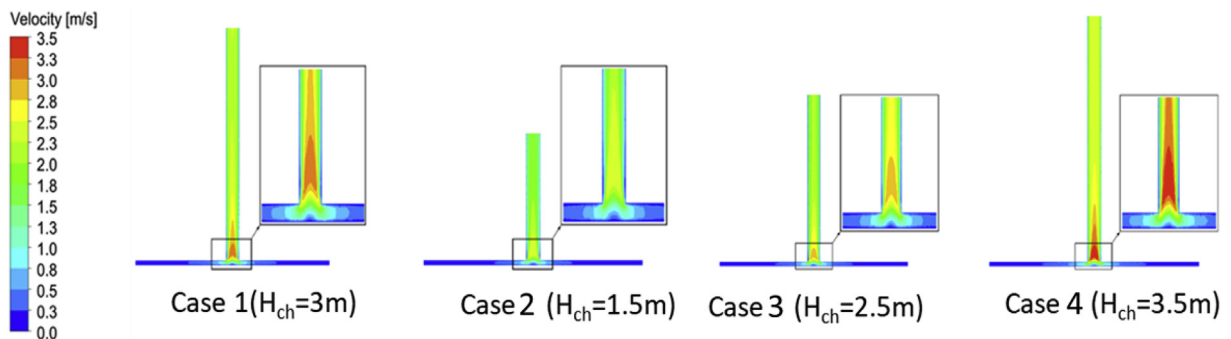

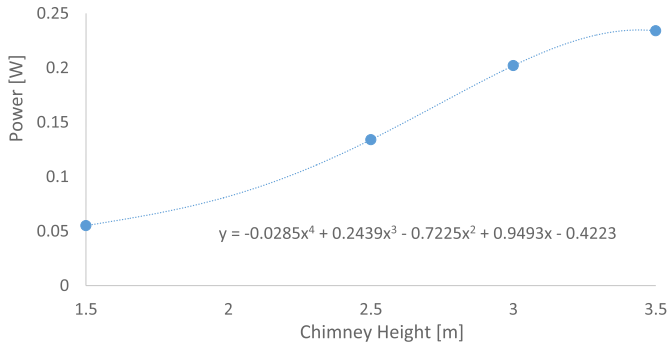**Fig. 10.** Velocity distribution for Case 1, Case 2, Case 3 and Case 4.

Fig. 11. Change of power of SCPP wrt chimney tower height.

which also can be concluded from equation (5). This critical point found is much smaller than the calculated maximum available height of the chimney, proposed by Zhou et al. (2009).

3.3. Influence of solar chimney radius on SCPP performance

In the following, simulation results based on different diameters of the solar chimney are presented. The diameter of the studied SCPP chimney is considered as, 20 cm (Case 4), 15 cm (Case 5), 25 cm (Case 6) and 35 cm (Case 7). The influence of the change of tower diameter on the temperature of the air flowing inside the chimney of the studied SCPP, is illustrated in Fig. 12. As it is shown in the figure, the maximum value of temperature exists at the base (on the absorber especially at the inlet of the tower) and minimum temperature value exists on the collector roof. It is clear that the tower diameter has a significant effect on temperature distribution, especially at the entrance of the chimney tower, where there will be a turbine.

From Fig. 13 (a) it can be seen that the air temperature inside SCPP increases with increasing tower diameter until reaching the best value (around 25 cm) and after that, the temperature starts to drop due to the requirement of high thermal power to heat large volume of chimney tower caused by the large diameter.

Fig. 13 (b) represents the influence of the SCPP tower diameter on the air velocity. It can be seen that the air velocity increases in the direction of the inlet to the center of the chimney. Also, it is clear that the air velocity decreases with increasing chimney diameter first, in which the air velocity reaches its maximum value at Case 5 and its minimum value at Case 7. This decrease of air velocity is caused by pressure change. The results show that the diameter of the tower has significant impact on the distribution of air velocity inside the tower, and it can be considered as an important parameter to improve the effectiveness of SCPP.

The variations in the tower diameter on the output power of SCPP is illustrated in Fig. 14. From results, it can be noted that increasing the diameter of the tower leads to an increase in the output power until reaching some specific value of tower diameter, which is considered as the best point.

After that value, output power starts to decrease, and from that point, it has an adverse impact on power and efficiency because the air temperature and the pressure difference decreases dominantly after that point. For this reason, the increase in the diameter of the chimney is limited by the power factor, and it is important for choosing the best diameter for the tower. When the results are compared with the work of Maia et al. (2009), temperature trends and velocity trends show similar properties, but power trends has not been evaluated in their work. According to the simulation results, best choice for the diameter of the tower is 30 cm in current study.

3.4. Effects of solar chimney geometry on SCPP performance

Based on Sections 3.1 and 3.2, it has been noted that the performance of SCPP is affected by the tower height and diameter. In the following parts, four different structures of chimneys that are usually used for the SCPP are analyzed in terms of their performance regarding air pressure, temperature and velocity. The chimney configurations considered are standard chimney (Case 6-a), diverging chimney (Case 6-b), converging-diverging chimney (Case 6-c), and standard-diverging chimney (Case 6-d).

Fig. 15 (a) represents the distribution of air temperature inside SCPP for different configurations of the tower. It can be seen that temperature distribution trends are same for all cases except the converging-diverging tower (Case 6-c), which has different temperature distribution, especially in the area at the end of collector near to tower entrance. Also, it is noticed that the standard tower (Case 6-a) has the highest air temperature throughout the collector diameter.

The distribution of air velocity inside SCPP for different tower configurations are displayed in Fig. 14(b). Results show that even trends of air velocity are similar for all configurations, the diverging tower (Case 6-b) has the maximum velocity compared to other configurations, and the converging-diverging tower (Case 6-c) has the lowest magnitude of air velocity. The outcomes indicate that changing the tower configuration has impacts on the air velocity thus effectiveness of the whole SCPP.

Fig. 16 illustrates the air velocity contours based on different tower configurations. It is clear that the most noticeable changes happen at the inlet of the tower which affects mostly on airflow velocity. Therefore design of this region is so important to increase the efficiency of SCPP. The contours indicate that the maximum air velocity appears at the entrance region of the tower for all cases,
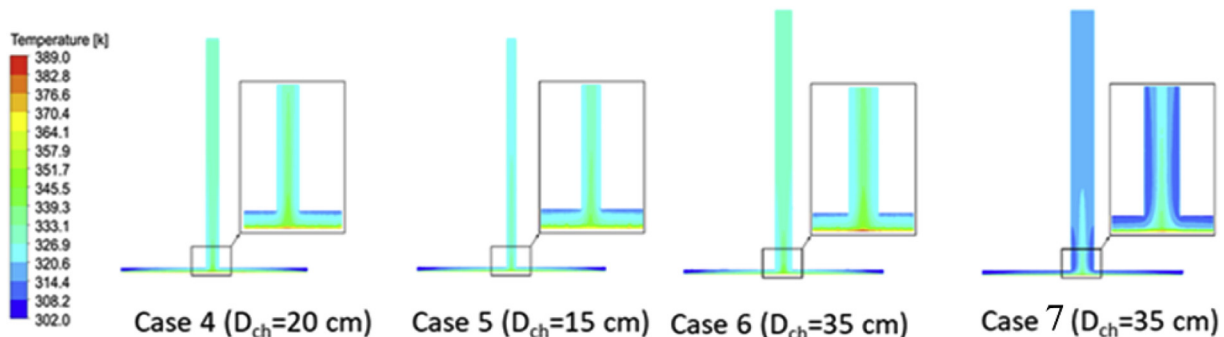

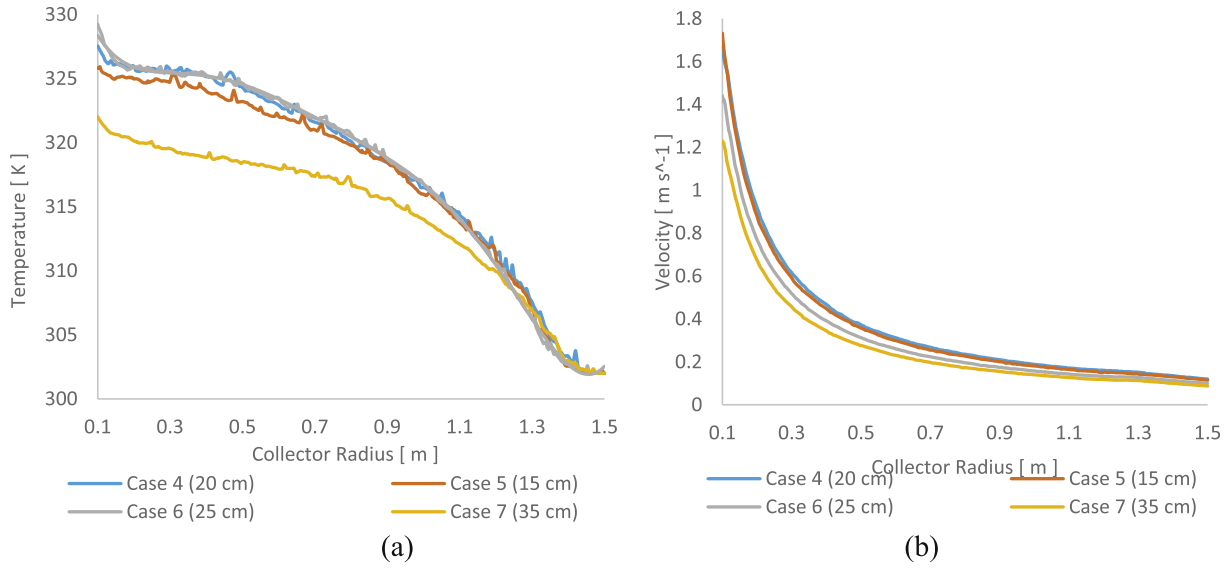**Fig. 12.** Air temperature distribution among various tower diameters.

Fig. 13. Effect of SCPP's tower diameter (a) Temperature profile (b) Velocity profile.
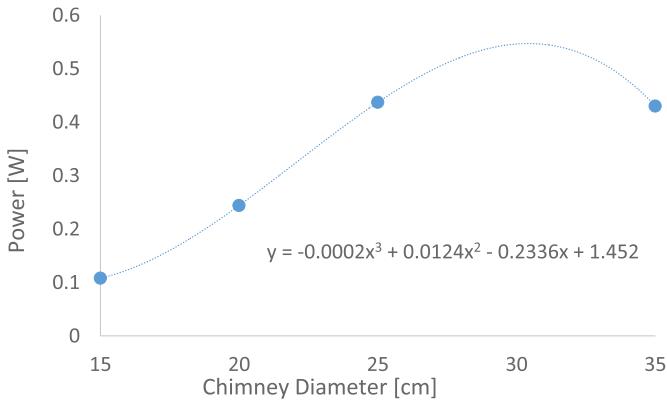

Fig. 14. Variation of power with respect to SCPP's tower diameter.

but the velocity gradient changes among the different configurations. For both the standard-diverging (Case 6-d) and diverging tower (Case 6-b), velocity is decreasing near the exit; but for standard (Case 6-a) and the converging-diverging (Case 6-c) tower, the velocity magnitude is almost same among the tower. Moreover, the area which has the maximum velocity near the tower inlet, also differs according to geometry and the maximum velocity region is at the diverging tower. Furthermore, the converging-diverging configuration (Case6-c) has the highest value of the velocity in the middle of the tower because of area reduction, and this is not advantageous for the turbine configuration.

For all considered geometries of different cases, maximum pressure difference occurs at the inlet of the tower, but among all configurations, maximum pressure difference happens in both the diverging tower (Case 6-b) and the standard-diverging tower (Case 6-d). The lowest pressure difference occurs in the converging-
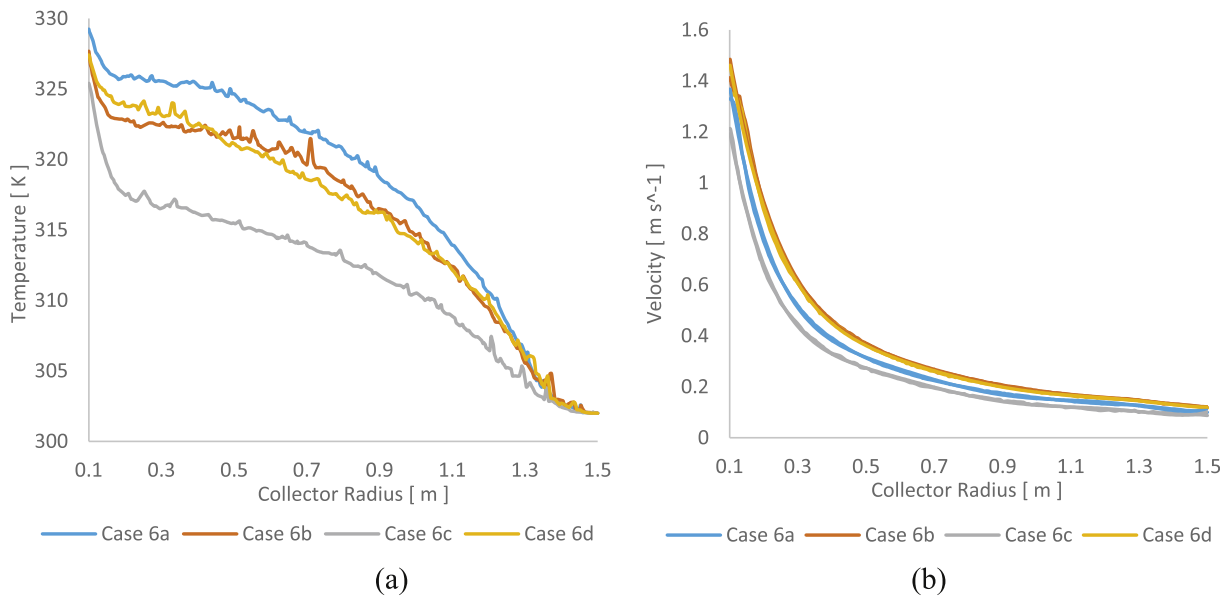

Fig. 15. The influence of different SCPP's tower configurations (a) Temperature profile (b) Velocity profile.
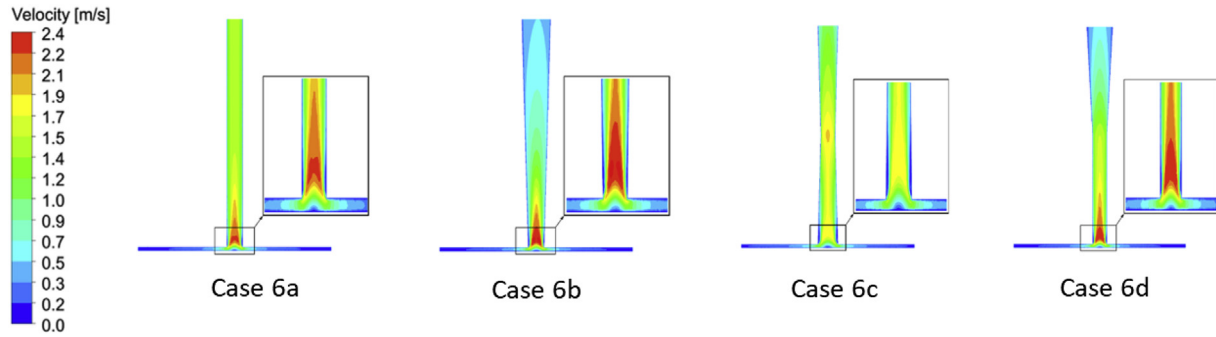
Fig. 16. The simulation results based on the different chimney configurations.

diverging tower (Case 6-c). The results confirm that the area at the inlet of the tower is significant for the flow, and it can have a significant effect on the magnitude of the velocity due to the pressure imbalance which produces the airflow inside the SCPP. Based on the above, choosing an appropriate design and configuration is an important factor for increasing the performance of SCPP.

The values of the output power of the SCPP for different tower configurations are presented in Table 6. The energy production which can be obtained from the turbine is proportional to the magnitude of the air velocity inside the SCPP. Therefore, the key to raise the value of the energy production is increasing the magnitude of the air velocity and thus the value of pressure difference. According to findings, it has been noted that the divergent tower (Case 6-b) is the best configuration for the best tower design due to its highest output power and relatively simpler geometry compared to other configurations of Cases 6-c and 6-d.

3.5. Effects of collector diameter on SCPP performance

In the following part, the impact of size of the solar collector diameter on the studied SCPP's performance is presented. According to Table 3, considered diameters for assessing the performance of the SCPP are 200, 250, 300, 350 and 400 cm, respectively.

The distribution of air temperature for different collector diameters is presented in Fig. 17. When results are examined, it is obvious that the maximum temperature exists at the absorber, lowest temperature at the entrance of the collector and air temperature starts to increase until reaching the maximum value at the entrance of the tower. It is noteworthy that, the temperature gradient increases by increasing the collector diameter.

The influence of changing SCPP collector diameter on the air temperature is presented in Fig. 18 (a). The results indicate that increasing collector diameter increases the temperature values. Moreover, the temperature distribution curve is similar for all diameters, and it increases by increasing the collector diameter until reaching the maximum collector diameter value, which is equal to 4 m.

The influence of the change of SCPP collector diameter on the air velocity is presented in Fig. 17 (b). The results show that the velocity of air is affected mostly by varying collector diameter. Moreover, the velocity profiles are the same for all considered cases, but the maximum value for each curve differs with increasing collector diameter; and at the point that collector diameter equals to 4 m
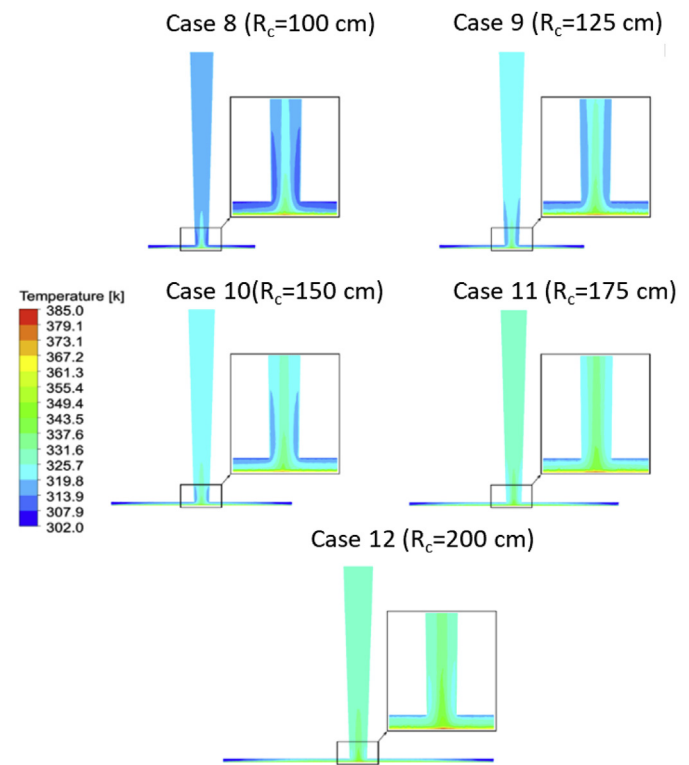

Fig. 17. The simulation results showing the air temperature distribution among chimneys with different collector dimensions.

(Case-12) it reaches to the highest air velocity. Thus, the diameter of the collector is one of the most important parameters which affects directly the performance of SCPP considering also the cost and the available area for construction.

The impact of changing the solar collector diameter on the output power of SCPP is illustrated in Fig. 19. According to the findings, it has been noted that there is an increase in the value of energy directly proportional to the increase in the diameter of the solar collector. It is also noticeable that the value of the output power of SCPP approaches stability when the value of the diameter of the solar collector reaches 4 m (Case-12). This is a supportive

Table 6
Variation of power with respect to SCPP's chimney configurations.

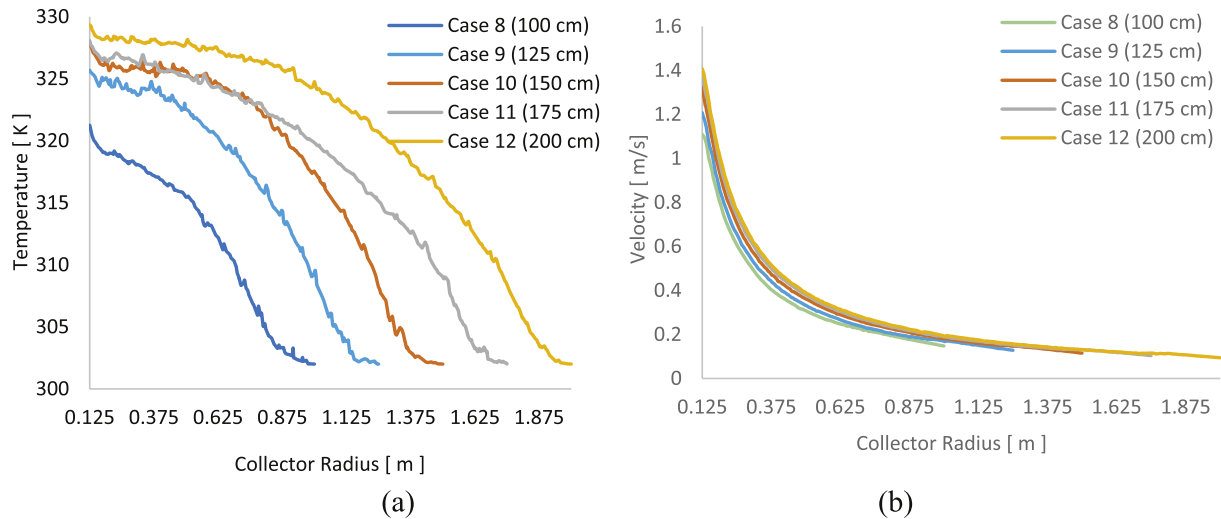|	Standard Chimney	Diverging Chimney	Converging-Diverging Chimney	Standard Diverging Chimney
Power [W]	0.41	0.54	0.42	0.49

Fig. 18. The influence of SCPP's collector diameter (a) On its temperature profile (b) On its velocity profile.

finding for considering the collector diameter regarding cost and the available area for construction is of importance.

Therefore, the SCCP collector with 400 cm diameter has better performance in terms of pressure difference to increase the temperature and velocity of the air for producing power. From the above, it can be concluded that increasing the diameter of the solar collector is of importance on the efficiency and effectiveness of the solar chimney system, and it can be considered as an essential and influential factor in increasing the value of output power of SCPP.

3.6. Effects of collector height on SCPP performance

The other parameter which has an effect on the performance of the SCPP is the height of the collector. In the following part, four different value is considered as the height of the SCPP's collector 4, 6, 8 and 10 cm, as shown in Table 3.

The influence of change in height of the SCPP's collector on the temperature of the flow is depicted in Fig. 20. From these contours, it can be noted that there are some changes present in temperature distribution through both the solar collector and the tower due to the effect of changing the height of the collector. The height of solar collector effects significantly on the heated area under the solar collector and also on area at the entrance of the tower.

From Fig. 21, it has been observed that the temperature distribution is similar for all cases except for collector height equal to 4 cm (Case-13). Also, the maximum air temperature differs from

one case to another, and it reaches its maximum value at collector height equal to 6 cm (case 12).

The influence of changing the height of the SCPP's collector on the temperature of the flow is depicted in Fig. 22. According to the findings, the value of the output power of SCPP can be affected by the change in the height of the solar collector. There is the best height where the value of the output power reaches its highest level; and further, it decreases by increasing the height of the solar collector. This indicates the importance of choosing an appropriate height for the solar collector, since there is found to be an optimum height of the collector for maximum power production, and a very tall collector is not advantageous. In this study, the best value of height of the solar collector is equal to 6 cm (Case-12), where the output power value reaches the highest.

3.7. Effects of the inclination angle of the collector on SCPP performance

In the following, the third collector parameter which can affect the performance of SCPP, is studied; which is the inclination angle of the solar collector. It is considered to be an effective one that can make a change in the performance of the SCPP. As written in Table 4, the studied inclination angles of the solar collector are considered as 0, 0.5,-0.5 and −1, respectively.

The changes in the temperature of the air flowing inside SCPP based on different inclination angles of the collector roof are presented in Fig. 23. The findings indicate the presence of the same temperature distribution inside the tower for all angles with little difference along with the collector. They also indicate the positive and negative angles affected the temperature distribution at the area in the entrance of the collector and also at the area near to the collector roof.

The distribution of air temperature inside SCPP for different inclination angles of the collector roof r is depicted in Fig. 24 (a). The temperature profiles show similarity in curves except Case 19, which has a reduction area at the inlet of the collector and that reduction area leads to some changes in the temperature profile. Furthermore, for cases 12-a, 12-b and 12-c the maximum temperature is almost the same for all of them; but the highest value of temperature compared to other angles belongs to Case-12 which has no inclination angle.

The distribution of the air velocity inside SCPP for different inclination angles of the SCPP's collector is displayed in Fig. 24 (b).
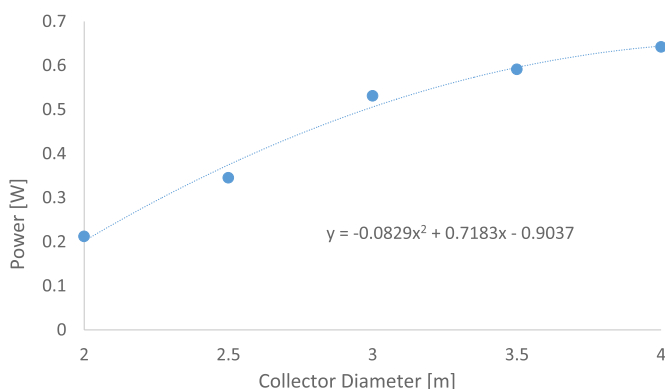

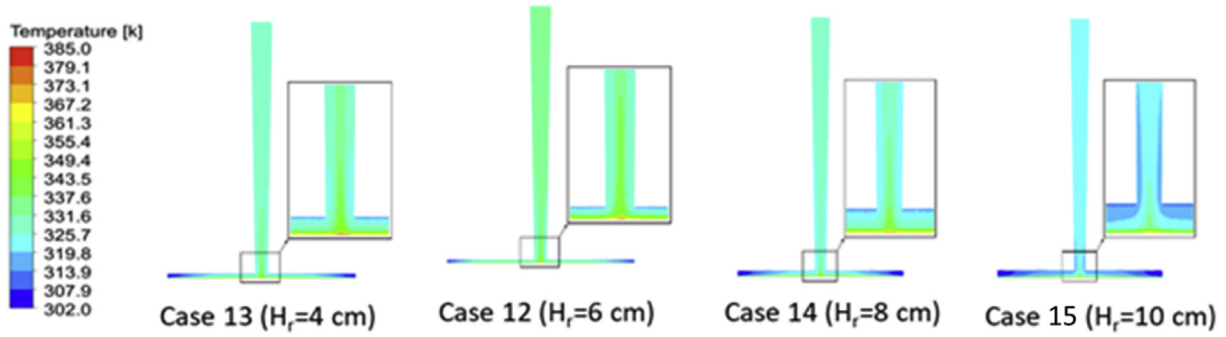**Fig. 19.** Variation of power with respect to SCPP's collector diameter.

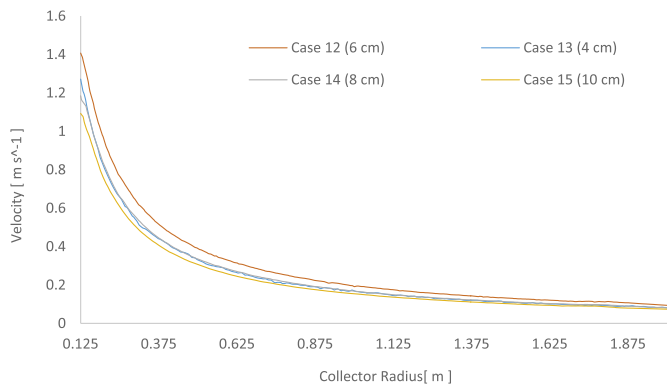**Fig. 20.** The simulation results for the air temperature distribution among various collector heights.

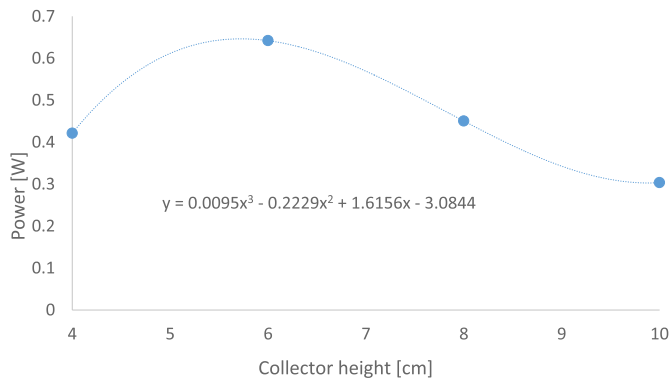**Fig. 21.** The influence of SCPP's collector height on the velocity profile.

Fig. 22. Variation of power with respect to SCPP's collector height.

The results indicate the existence of a difference in temperature profiles starting from the entrance of the collector until reaching the end. These changes belong to the impact of collector roof angles on velocity magnitude along the collector; and it leads to differences in the value of maximum velocity for each case and it reaches the highest value at Case (12-b) and minimum value at Case (12-a). According to above, it can be concluded that, the inclination angle of the SCPP's collector has an essential effect on the velocity magnitude of the airflow.

The influence of changing the inclination angle of the collector on the output power of SCPP is illustrated in Fig. 25. The findings showed that the output power of the SCPP is influenced by changing the inclination (tilt) angle of the solar collector roof. Moreover, the inclination angle of the collector equal to 0 (Case-12) is the best choice where the output power reaches its maximum

value. Furthermore, the results show the importance of the inclination angle of the solar collector roof for the performance and effectiveness of the solar chimney systems.

4. Model to prototype: engineering interpretation

Experimental study of a full-scale solar chimney prototype is unlikely to be done since a moderate power plant is minimum 100 m in height. So the small scale model presented in this study is proposed to be used for testing and design of the prototype by a similarity scaling. With successfully developing a valid model, it is possible to predict the performance of the prototype under certain conditions. The dimensional analysis methodology focuses on combining the effects of various variables into fewer dimensionless variables, thereby scaling the variables to exhibit similar effects on the different physical models (Toghraie et al., 2018).

For a complete similarity; geometric similarity which ensures each dimension must be scaled by the same factor, kinematic similarity which ensures velocity at any point in the model must be proportional and dynamic similarity which ensures all forces in the model flow is scaled by a constant factor to corresponding forces in the prototype flow; should be attained. For SCPP studies, according to Koonsrisuk and Chitsomboon (2007), both geometric and dynamic similarity can be achieved for a SCPP.

Dependence of the kinetic power (maximum power available for the turbine), on the independent variables is proposed by the equation seen below. It is important to note that a solar chimney system without a turbine is considered as it is given in Eq (14) (Koonsrisuk and Chitsomboon, 2009):

$$\rho A V^2 = f^n \left(\rho, g, \frac{q'''}{C_p}, \beta, h_c \right) \tag{14}$$

where volumetric thermal expansion coefficient is (Patel. et al., 2014);

$$\beta = -\frac{1}{\rho} \left(\frac{\partial \rho}{\partial T} \right)_\rho \tag{15}$$

Heat flux can be characterized as following (Koonsrisuk and Chitsomboon, 2009):

$$(q''A_r) = \dot{m} C_p \Delta T \tag{16}$$

The functional relationship is found by Buckingham Pi theorem to be (Koonsrisuk and Chitsomboon, 2009);

$$\frac{\frac{1}{2}\dot{m}V^2}{\rho h_c^{3.5} g^{1.5}} = f^n \left(\frac{q''A_r \beta}{\rho C_p h_c^{5/2} g^{1/2}}, \frac{r_c}{h_c}, \frac{h_r}{h_c} \right) \tag{17}$$
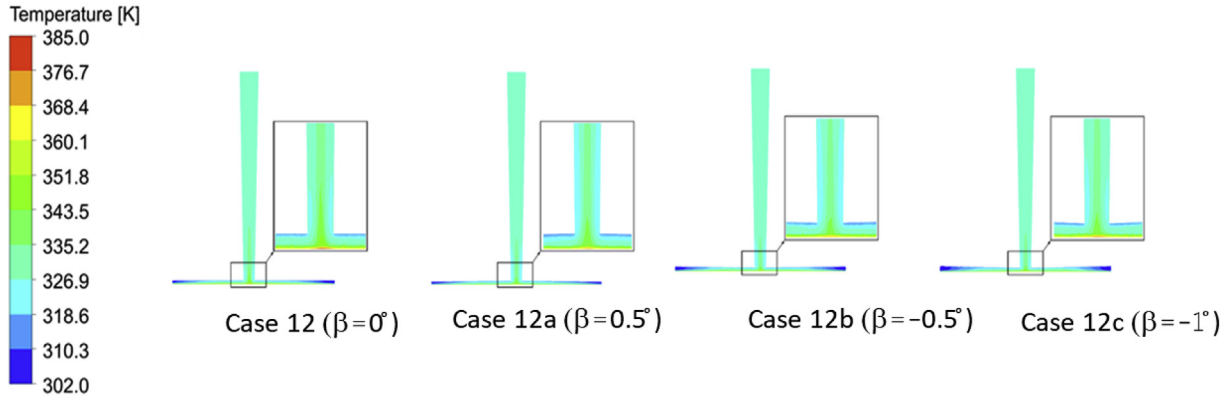
Fig. 23. The simulation results for the air temperature distribution among various collector inclination angles of the SCPP for cases 12 to 12-c.
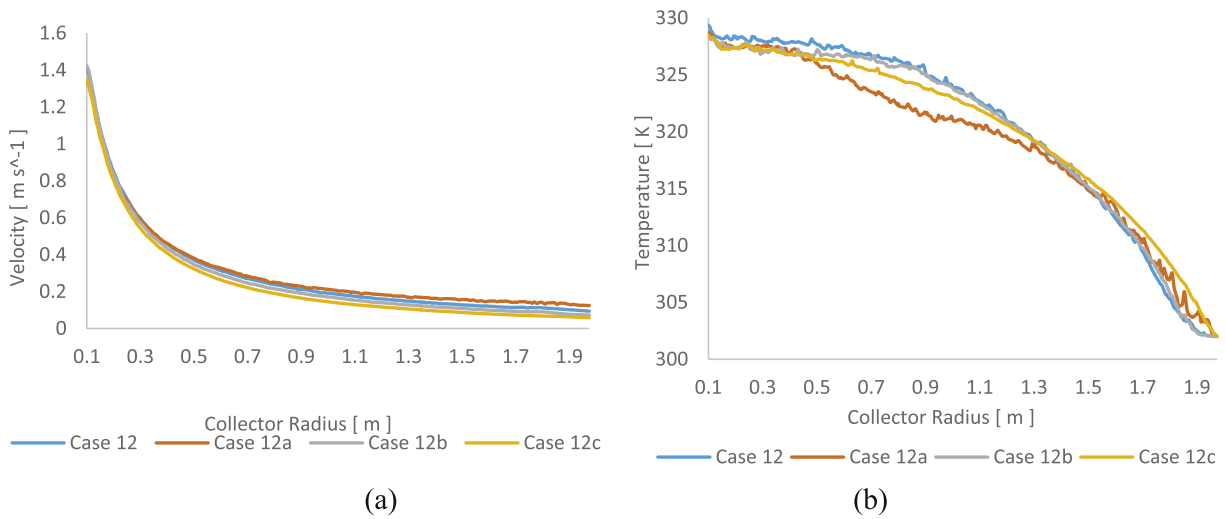

(a)

(b)

Fig. 24. The influence of SCPP's collector inclination angle on (a) Temperature distribution (b) Velocity profile.
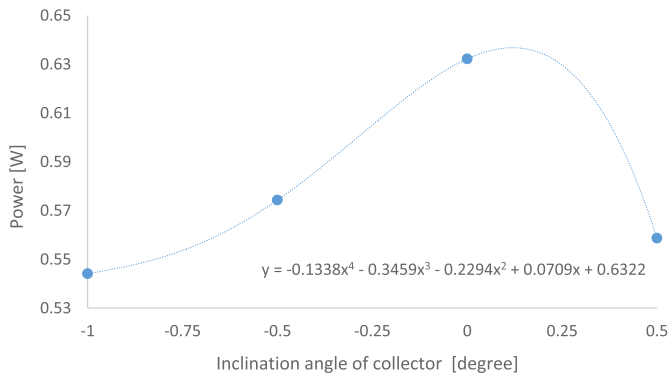

Fig. 25. Variation of power with respect to inclination angle of the SCPP collector.

So by further observation and calculations, the similarity requirements are such that:

For geometric similarity;

$$\frac{h_{ch,p}}{h_{ch,m}} = \frac{r_{ch,p}}{r_{ch,m}} = \frac{h_{coll,p}}{h_{coll,m}} = L_r \tag{18}$$

For kinematic similarity;

$$\frac{V_p}{V_m} = \frac{\sqrt{h_{chp}}}{\sqrt{h_{chm}}} \frac{\sqrt{\beta_m}}{\sqrt{\beta_p}} = f^n(L_r) \tag{19}$$

And finally for dynamic similarity assuming constant heat flux, it can be interpreted that (Koonsrisuk and Chitsomboon, 2009);

$$\frac{r_{r,m}}{r_{r,p}} = \left(\frac{h_{c,m}}{h_{c,p}}\right)^{5/4} \tag{20}$$

For maximum turbine power scale ratio, combining equations (5) and (6), and further simplification, it can be found that;

$$P_r = \frac{P_p}{P_m} = f^n\left(L_r^{3.5} \cdot \frac{\Delta T_p^{1.5}}{\Delta T_m}\right) \tag{21}$$

This relationship shows that power ratio scales with the geometric similarity ratio to the power of 3.5 and with the temperature difference ratio to the power of 1.5. For determination of the function, experimentations should be done to correctly analyze the relationship. Chitsomboon and Koonsrisuk (Koonsrisuk and Chitsomboon, 2009) verified by experimentations and simulations, that;

$$\frac{1}{2}\dot{m}V^2 = \frac{q'''A_r\beta}{C_p}gh_c \tag{22}$$

So the power scale factor for modelling SCPP can be found regarding the power required as;

$$P_r = \frac{P_p}{P_m} = L_r^{3.5} \cdot \frac{\Delta T_p}{\Delta T_m}^{1.5} \cdot \frac{\beta_p}{\beta_m} \tag{23}$$

So far, by the correct selection of the dominant performance parameter which can be done by correctly interpreting the results of this study considering simulation of so many different alternatives, "the best" design of a real scale SCPP prototype can be done for maximum power requirement.

5. Conclusion

This study investigates geometric parameters' effects and different configurations' effects on SCPP performance, simultaneously and additively, and in a more detailed way compared to other small scale SCPP studies in literature. It introduces an insight to the performance enhancement methods and finding the best configuration of a SCPP model, which will be the basis of a detailed prototyping process for maximum output power of a real scale chimney considering all parameters effects. This study also offers a better understanding of the nature of the impact of these parameters on the performance of SCPP. The most important results obtained in this study are given below:

- The performance of the SCPP increases by increasing the height of the chimney up to a specific point of height. If the height increases more than that point, the performance of the SCPP rises slightly, then starts to fall. According to the obtained results, the best performance was achieved from the SCPP with 3.5 m chimney height. Based on the simulation results for the proposed case, the pressure value is less than the others while the velocity and temperature were higher than the others. It can be concluded that there is a feasible height value, which can be determined for a good cost-performance depending on numerical simulations and the trend of the power curve. Since the turbine power is directly related to maximum velocity in chimney and velocity is related to chimney height and the temperature difference to the power 0.5. This maximum height parameter for the chimney is realized to be less than the maximum height parameter calculated by Xhou et al. (Zhou et al., 2009) in their study. In this study, an optimum chimney height is proposed considering also the cost of chimney and the influence of the chimney height parameter on the performance of SCPP.
- The study of changing the diameter of the SCPP's chimney which has a significant influence on SCPPs performance, shows that there is an optimum diameter value. By increasing the chimney tower diameter, the performance of the SCPP increases; but if the chimney diameter increases more than critical tower diameter (optimum value), then it has a negative impact on the performance of the SCPPs. By observation of different simulations, chimney diameter is found to have the maximum impact on the performance of the SCPP. Considering nondimensionalization for the prototyping, this parameter is proposed to be used as the geometric scaling factor for experimental studies. According to the obtained results, the best performance was achieved from the tower diameter of 30 cm.
- Analyzing the geometry of the SCPP's tower is considered as one of the best methods to find a way for increasing the efficiency of

SCPP. The different structures of the chimney can result changes in the power and performance of SCPPs. According to the proposed simulation results, the diverging chimney (Case 6-b) has the best performance compared to the others, as explained in the previous parts.
- Besides the tower, the SCPP's collector dimensions have a considerable effect on the performance. In this research, three features of the SCPPs' collectors: height, diameter and inclination angle of the collector are analyzed and simulated. It is found that all three have a direct influence on the efficiency. According to the obtained simulation results, the collector with 400 cm diameter, decreased the pressure and increased the flow velocity and temperature better than the other ones, by causing improvement in the performance of the SCPP. It can also be concluded that as long as cost performance is considered and there is enough space, the collector diameter value can be increased for a better performance, since power of turbine is related to the heat gain, and heat gain is directly related to the area of the collector.
- Furthermore, the collector height is found to have an important effect, and there is a best value of height for the best performance, which can be found by numerical simulations, and later to be used for best design of the prototype by using the correct scaling methodology. According to the obtained simulation results, the collector with 6 cm height has the best performance.
- The results of simulation of the inclination angle of the studied SCPP show that the collector with zero inclination angle (Case-12) has better performance compared to the others.
- By the correct selection of the dominant performance parameter which can be done by correctly interpreting the results of this study, "the best" design of a SCPP real scale prototype considering maximum power requirement can be done. The gained research results will contribute to further understanding of the geometrical parameters' effect on solar chimney performance in order to generate emission-free clean power.

CRediT authorship contribution statement

Ekin Özgirgin Yapıcı: Conceptualization, Methodology, Writing - original draft, Supervision, Writing - review & editing. **Ece Ayli:** Visualization, Investigation, Supervision, Validation, Writing - original draft, Writing - review & editing. **Osama Nsaif:** Formal analysis, Investigation, Data curation, Writing - original draft.

Declaration of competing interest

The authors declare that they have no known competing financial interests or personal relationships that could have appeared to influence the work reported in this paper.

Appendix A. Supplementary data

Supplementary data to this article can be found online at https://doi.org/10.1016/j.jclepro.2020.122908.

References

Al-Dabbas, A.M., 2011. Performance analysis of solar chimney thermal power systems. Therm. Sci. 15 (3), 619–642.

Al-Kayiem, H.H., Aja, O.C., 2016. Historical and recent progress in solar chimney power plant enhancing technologies. Renew. Sustain. Energy Rev. 58, 1269–1292.

Amudam, Y., Chandramohan, V.P., 2019. Influence of thermal energy storage system on flow and performance parameters of solar updraft tower power plant: a three-dimensional numerical analysis. J. Clean. Prod. 207, 136–152.

Bernardes, M.D.S., Voß, A., Weinrebe, G., 2003. Thermal and technical analyses of

solar chimneys. Sol. Energy 75 (6), 511–524.

Bouabidi, A., Ayadi, A., Nasraoui, H., Driss, Z., Abid, M.S., 2018. Study of solar chimney in Tunisia: effect of the chimney configurations on the local flow characteristics. Energy Build. 169, 27–38.

Cao, F., Liu, Q., Yang, T., Zhu, T., Bai, J., Zhao, L., 2018. Full-year simulation of solar chimney power plants in Northwest China. Renew. Energy 119, 421–428.

Dai, Y.J., Huang, H.B., Wang, R.Z., 2003. A case study of solar chimney power plants in Northwestern regions of China. Renew. Energy 28 (8), 1295–1304.

Fallah, S.H., Valipour, M.S., 2019. Evaluation of solar chimney power plant performance: the effect of artificial roughness of collector. Sol. Energy 188, 175–184.

Fasel, H.F., Meng, F., Shams, E., Gross, A., 2013. CFD analysis for solar chimney power plants. Sol. Energy 98, 12–22.

Fathi, N., McDaniel, P., Aleysain, S., Robinson, M., Vorobieff, P., Rodriguez, S., Oliveira, C., 2018. Efficiency enhancement of solar chimney power plant by use of waste heat from nuclear power plant. J. Clean. Prod. 180, 407–416.

Fluent, ANSYS Fluent Theory Guide- FLUENT 18.2.

Ghalamchi, M., Kasaeian, A., Ghalamchi, M., Mirzahosseini, A.H., 2016. An experimental study on the thermal performance of a solar chimney with different dimensional parameters. Renew. Energy 91, 477–483.

Hu, S., Leung, D.Y., Chan, J., 2017. Numerical modelling and comparison of the performance of diffuser-type solar chimneys for power generation. Appl. Energy 204, 948–957.

Koonsrisuk, A., Chitsomboon, T., 2007. Dynamic similarity in solar chimney modeling. Sol. Energy 18 (12), 1439–1446.

Koonsrisuk, A., Chitsomboon, 2009. T Partial geometric similarity for solar chimney power plant modelling. Sol. Energy 83 (9), 1611–1618.

Li, J.Y., Guo, P.H., Wang, Y., 2012. Effects of collector radius and chimney height on power output of a solar chimney power plant with turbines. Renew. Energy 47, 21–28.

Li, J., Guo, H., Huang, S., 2016. Power generation quality analysis and geometric optimization for solar chimney power plants. Sol. Energy 139, 228–237.

Maia, C.B., Ferreira, A.G., Valle, R.M., Cortez, M.F., 2009. Theoretical evaluation of the influence of geometric parameters and materials on the behavior of the airflow in a solar chimney. Comput. Fluid 38 (3), 625–636.

Najm, O.A., Shaaban, S., 2018. Numerical investigation and optimization of the solar chimney collector performance and power density. Energy Convers. Manag.

168, 150–161.

Nasraoui, H., Driss, Z., Kchaou, H., 2020. Novel collector design for enhancing the performance of solar chimney power plant. Renew. Energy 145, 1658–1671.

Ninic, N., Nizetic, S., 2007. Solar Power Plant with Short Diffuser. Patented Invention. PCT/HR2007/000037-(WO/2009/060245).

Nizetic, S., 2011. Technical utilization of convective vortices for carbon-free electricity production: a review. Energy 36, 1236–1242.

Nizetic, S., Penga, Z., Arici, M., 2017. Contribution to the research of an alternative energy concept for carbon free electricity production: concept of solar power plant with short diffuser. Energy Convers. Manag. 148, 533–553.

Okoye, C.O., 2016. A Two-Stage Feasıbılıty Approach for Solar Chımney Power Plant Desıgn, MSc Thesis, Mıddle East Technıcal Unıversıty Northern Cyprus Campus (Turkey).

Patel, A.K., Prasad, D., Ahmet, M.R., 2014. Computational studies on the effect of geometric parameters on the performance of a solar chimney power plant. Energy Convers. Manag. 77, 424–431.

Penga, Z., Nizetic, S., Arici, M., 2019. Solar plant with short diffuser concept: further improvement of numerical model by included influence of guide vane topology on shape and stability of gravitational vortex. J. Clean. Prod. 212, 353–361.

Thakre, S.B., Bhuyar, L.B., Dahake, S.V., Wankhade, P., 2013. Mathematical correlations developed for solar chimney power plant "A critical review. Global J. Res. Eng. 13 (1).

Toghraie, D., Karami, A., Afrand, M., Karimipour, A., 2018. Effects of geometric parameters on the performance of solar chimney power plants. Energy 162, 1052–1061.

Wilcox, D.C., November 2006. Turbulence Modelling for CFD, third ed. DWC Industries.

Zhou, X., Yang, J., Xiao, B., Hou, G., 2007. Simulation of a pilot solar chimney thermal power generating equipment. Renew. Energy 32 (10), 1637–1644.

Zhou, X., Yang, J., Xiao, B., Hou, G., Xing, F., 2009. Analysis of chimney height for solar chimney power plant. Appl. Therm. Eng. 29 (1), 178–185.

Zuo, L., Liu, Z., Ding, L., Qu, N., Dai, P., Xu, B., Yuan, Y., 2020. Performance Analysis of a Wind Supercharging Solar Chimney Power Plant Combined with Thermal Plant for Power and Freshwater Generation, vol. 204. Energy Conversion and Management, pp. 11–28.